Glenohumeral contact force, peak muscle forces, and thorax motion increase with fatiguing wheelchair propulsion in persons with a spinal cord injury

de Vries, W. H.K.; Bossuyt, F. M.; Veeger, H. E.J.; Arnet, U.

DOI
10.1016/j.jbiomech.2025.112651

Publication date
2025

Document Version
Final published version

Published in
Journal of Biomechanics

Journal of Biomechanics 184 (2025) 112651

Contents lists available at ScienceDirect

Journal of Biomechanics

journal homepage: www.elsevier.com/locate/jbiomech

Glenohumeral contact force, peak muscle forces, and thorax motion increase with fatiguing wheelchair propulsion in persons with a spinal cord injury

W.H.K. de Vries [a], F.M. Bossuyt [b], H.E.J. Veeger [c,*], U. Arnet [a]

[a] Upper Extremity Health Group, Swiss Paraplegic Research, Guido A. Zächstrasse 4, 6207 Nottwil, Switzerland
[b] Institute for Biomechanics, Department of Health Sciences and Technology, ETH Zürich, Hönggerberg, 8093 Zürich, Switzerland
[c] Department of Biomechanical Engineering, Delft University of Technology, Mekelweg 2, 2628 CD Delft, the Netherlands

ARTICLE INFO

Keywords:
Shoulder problems
Manual wheelchair users
Spinal cord injury
Fatigue
Shoulder load

ABSTRACT

Shoulder problems are highly prevalent among manual wheelchair users with spinal cord injury, affecting their functioning and quality of life. This study investigates the impact of fatigue on wheelchair propulsion technique and shoulder loading in manual wheelchair users (MWU) with SCI. Twelve MWU with a paraplegia performed a standardized fatiguing wheelchair propulsion protocol; a biomechanical assessment of treadmill propulsion was obtained before and after the fatiguing protocol. Rate of perceived exertion (RPE), upper extremity kinematics, and wheelchair propulsion kinetics were assessed. Results showed increased RPE post-fatigue, with no significant changes in exerted forces but increased thorax forward lean and range of motion. Musculoskeletal modelling showed elevated glenohumeral joint contact force and muscle forces post-fatigue. These findings suggest a potential link between fatigue, altered propulsion technique, and increased shoulder loading, highlighting the risk of overuse injuries. Moreover, increased thorax motion during propulsion may indicate fatigue onset. Prospective cohort studies are warranted to validate the presented findings and explore the relationship between shoulder loading and injury risk. Understanding these dynamics can inform interventions to mitigate shoulder pain and enhance the well-being of MWU with SCI.

1. Introduction

Shoulder pain has a high prevalence in manual wheelchair users (MWU) with a spinal cord injury (SCI) (Bossuyt et al., 2018; Gironda et al., 2004). The occurrence of shoulder pain detrimentally affects functioning, independence, participation, and quality of life (Eriks-Hoogland et al., 2011; Gutierrez et al., 2007; Jensen et al., 2005; Turner et al., 2001). Especially the muscles and tendons of the rotator cuff appear to be most affected in MWU with a SCI, in both pain and no-pain groups (Arnet et al., 2022). With the increased life-expectancy in persons with SCI, (Chamberlain et al., 2015; Strauss et al., 2006) there is an emerging need to understand intrinsic changes in soft-tissues over time, and how this influences the development of chronic tendon degeneration.

Despite the higher risk of shoulder overuse injuries in MWU with SCI and an almost 10-times higher risk of rupturing their supraspinatus compared with the general population (Akbar et al., 2010), MWU have only limited opportunities for recovery as they depend on their shoulders for all aspects of daily life. This combination of high-intensity-use and lack of opportunities for recovery appears to be a major factor in the high prevalence of shoulder pain. Risk of overuse might be related to peak loading during weight relief lifts (van Drongelen et al., 2011) or transfers (Gagnon et al., 2008). In addition, the repetitive (although with lower intensity) loading of the upper extremities during manual wheelchair propulsion (Lin et al., 2004; Rodgers et al., 1994; Veeger et al., 2002) could play an important role in the injury mechanisms as this might lead to local muscle fatigue (Qi et al., 2021) and a consequential temporary decrease in capacity. Indeed, acute tendon adaptations have been observed following fatiguing wheelchair propulsion (Bossuyt et al., 2020b) and may play a role in the injury mechanism. Fatigue could also be associated with changes in propulsion technique, leading to a different muscle load profile with potentially harmful effects.

Despite the long history of research on propulsion technique in

* Corresponding author.
E-mail address: h.e.j.veeger@tudelft.nl (H.E.J. Veeger).

https://doi.org/10.1016/j.jbiomech.2025.112651
Accepted 24 March 2025
Available online 28 March 2025

manual wheelchair propulsion, little is known on the effects of fatigue on shoulder loading. Rodgers et al.(Rodgers et al., 1994) studied the changes in movement patterns during a submaximal exercise test to exhaustion and reported that subjects propelled with greater trunk flexion when fatigued. Furthermore, changes with regards to timing have been reported. Here, start-up propulsion changed with an increase in push time (Rice et al., 2009) and a decrease in push angle, these changes have also been observed in steady state propulsion following fatigue and have been associated with compensatory changes in muscular activation (Bossuyt et al., 2020a). Qi et al.(Qi et al., 2021) studied changes in muscle activity with fatigue and reported a joint stiffening due to fatigue. Whether the observations on kinematic (Rodgers et al., 1994), kinetic or muscle activity(Rice et al., 2009) changes do imply an increase in shoulder load and thus a potential increase in injury risk due to fatigue, warrants additional research using a musculoskeletal model. Although musculoskeletal modelling has previously been used as a tool for the estimation of muscle forces in wheelchair propulsion (Dubowsky et al., 2008; Holloway et al., 2015; Leving et al., 2018; Lin et al., 2004; Veeger et al., 2002), no studies to date have studied the effect of fatigue-related effects on loading of the anatomical structures of the shoulder.

The aim of this study was to measure alterations in wheelchair propulsion technique and analyse changes in shoulder load under fatigue conditions by administering a standardized fatiguing-inducing wheelchair propulsion protocol to MWU with SCI. It was hypothesized that fatigue induced by the protocol would result in modifications to both propulsion technique as well as to the forces involved in wheelchair propulsion, potentially increasing load on the rotator cuff. This would be presented as increased rotator cuff forces and an elevated glenohumeral joint contact load calculated using musculoskeletal modelling.

2. Methods

2.1. Participants

All subjects provided written informed consent before participation in this study. Ethical approval was granted by the Ethikkommision Nordwest-und Zentralschweiz (project ID: 2017–00355). The study population included twelve community dwelling persons with a SCI, who are independent in manual wheelchair ambulation. In-depth detail on the recruitment and study procedures has been reported previously (Bossuyt et al., 2020a) and are briefly detailed below.

From the 12 participants 10 were male and 2 were female. Average age was 50.4 (SD 10.3) years, height was 1.72 (0.07) m and weight 72.9 (16.1) kg. Three persons had a lesion level between T2-T6, five had a lesion between T7 and T12, and four had a lesion at L1 or L2. Nine persons had a complete lesion, while mean time since injury was 26.3 (SD 11.5) years. Participants reporting shoulder pain that limited them in wheelchair propulsion, or joint fractures or dislocations still causing problems, were excluded.

2.2. Test procedure

Subjects performed an overground figure-8 wheelchair propulsion fatiguing protocol conform Collinger et al. (Collinger et al., 2010). The figure-8 protocol consisted of three times 4 min of wheelchair propulsion on a concrete floor, starting and stopping in the middle, and making respectively a left and a right turn around two pylons 18 m apart, for as many laps as possible to ensure high intensity and resulting fatigue (See Fig. 1).

Before and directly after the wheelchair fatiguing protocol participants propelled on a motorized treadmill (belt area 250 X 120 cm, Bonte Technology B.V., Groningen, Netherlands) for 40 sec at 4 km/h, corresponding to daily life speed of steady state propulsion. Participants rolling resistance was determined during initial measurements by a drag test, and extra resistance was added via a pulley system, to reach the desired power outputs of 25 W and 45 W. Rate of perceived exertion (RPE) was collected using a 20-point Borg scale, before and after each wheelchair propulsion task.

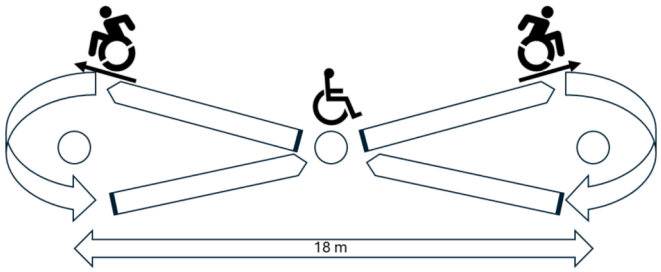

Fig. 1. Illustrating the fatiguing protocol consisting of overground wheelchair propulsion in a Fig. 8. Start and stop in the middle, making left and right turns around two pilons 18 m apart.

2.3. Data collection

During the treadmill propulsion tasks, wheelchair propulsion kinetics (WCP-kinetics) and upper extremity kinematics (UE-kinematics) of the participant's non-dominant side were recorded over a period of 30 s. The non-dominant side was tested under the assumption this shoulder would be most impacted by fatigue.

2.3.1. UE-kinematics

UE-kinematics were registered at 100 Hz with an eight-camera motion capture system (Qualisys, Gothenburg, Sweden). Subjects were equipped with reflective marker clusters, placed on the thorax, scapula (flat part of the acromion), humerus, forearm and hand (Karduna et al., 2001; McClure et al., 2001; Meskers et al., 2007; van Andel et al., 2008) (Fig. 2). Additional markers were placed on the wheelchair wheel axis and wheelchair frame, to enable the identification of the position of hand contact with respect to the wheelchair-rim. During initial measurements the position of bony landmarks (BLM) for the construction of anatomical reference frames conform (Wu et al., 2005) were indicated with a pointer, with respect to the segment's marker clusters. Using these initial measurements, BLM trajectories were calculated for the experimental settings from the marker clusters. BLM trajectories were bidirectionally filtered with 4th order low pass butterworth filter at 10 Hz; consequently, segment orientations were calculated according to the proposal by Wu et al (Wu et al., 2005). Thorax position and orientation, and joint angles between Scapula-thorax, humerus-thorax, forearm-humerus, and hand-forearm were used as input for the Delft Shoulder and Elbow Model (DSEM). As no marker cluster can be placed on the clavicle without significant influence of skin motion, joint angles of the clavicula are calculated by the DSEM conform Bolsterlee et al. (Bolsterlee et al., 2014).

2.3.2. WCP-kinetics

For all experimental conditions, participants used their own wheelchair. WCP-temporal and kinetics variables such as push-time, cycle-time, contact angles, and exerted forces and moments at the rim were collected with a Smartwheel (24 in.; Three Rivers Holdings, Inc, Mesa, AZ, USA), at the measured non-dominant side with a sample frequency of 240 Hz. The wheel at the other side was replaced with a dummy wheel having the same inertial. Smartwheel and motion capture equipment were electronically synchronized. Besides UE-Kinematics, exerted forces and moments delivered by the hand to the rim were used as input for the DSEM. Hand moment was calculated as the difference between total moment as measured at the wheel-axis and propulsive moment as calculated by multiplication of the tangential force at the rim with rim radius, for the push-phase defined by hand contact (van der Linden et al., 1996; Veeger et al., 2002).

Fig. 2. The setup for the registration of UE-kinematics and WCP-kinetics, before and after the overground fatiguing protocol. A pulley system was used to add extra weight to arrive at 25 W or 45 W power output for all participants. For each participant, the required weights were determined from a drag test measuring rolling resistance force.

2.4. Data processing

For each experimental condition (pre and post fatigue wheelchair propulsion on a treadmill at 4 km/h, at 25 W or 45 W), marker and Smartwheel data of ten consecutive pushes were selected, scaled to the average push duration, and averaged per participant. In case of left-handed measurements all 3D data were mirrored in the sagittal plane to enable processing with the musculoskeletal model, which consists of a right shoulder only. Push start and end angles were defined as the position of a marker on the base of the third metacarpal of the hand at the onset and end of the recorded propulsion moment. The angles were expressed relative to the wheel top dead center. Push time and cycle time were based on the instants of moment onset, end, and the instant of the next push moment. For propulsive moment a threshold of 2 NM was used, just above the noise level of the system used.

2.5. Musculo-skeletal model

To analyze shoulder load, the averaged UE-kinematics and WCP-kinetics of each subject were input to the DSEM (Nikooyan et al., 2011). The DSEM is a large-scale inverse-dynamics based finite element model in which anatomical structures are modelled by mechanical elements (van der Helm, 1994a, b). It includes all bones, joints, and most ligaments of the shoulder (with a total of 17-DOF) as well as 31 muscles divided into 139 muscle elements. This comprehensive geometry was measured from cadaveric datasets (Veeger et al., 1991; Veeger et al., 1997). Muscle elements are modelled as a three-component Hill type model consisting of a second-order activation dynamics part and a first-order contractile dynamics part (Nikooyan et al., 2011). Thorax position and orientation, and joint angles of the scapula and upper extremity serve as input for the model, as well as exerted forces and moments of the hand. From this input, scapular orientations are optimized by the model so the scapular medial border stays attached to the thorax and the conoid ligament stays at equal length (Nikooyan et al., 2011; van der Helm, 1994a, b). Subsequently, the clavicular orientation is calculated by the model conform (Bolsterlee et al., 2014), based on scapula position and orientation.

Furthermore, the joint moments are calculated by inverse kinematics, from segment kinematics and external forces and moments at the hand. The optimization of individual muscle forces to produce these joint moments has four constraints:

1. Muscle-force can only be positive (muscles can only pull);

2. the force that can be produced by each muscle at each instant of time, which is a function of the optimum fiber length, the physiological cross-sectional area and maximum muscle stress per $cm^{\hat{}}2$;

3. an energy cost function (Praagman et al., 2006);

4. a force direction constraint, to guarantee that the resulting joint contact force at the glenohumeral joint is directed into the glenoid of the scapula.

The DSEM has been validated against EMG during wheelchair propulsion and with an instrumented shoulder joint prothesis for several standardized tasks (Nikooyan et al., 2010; van der Helm, 1994b; van der Helm and Veeger, 1999).

From the full set of modelling results, peak glenohumeral (GH) joint moment and peak GH power, peak elbow moment and power, the peak GH joint contact force and the calculated peak forces of the rotator cuff muscles, deltoids, biceps and triceps were selected for further analysis.

The total of GH contact force was calculated by the vector summation of the model-estimated muscle forces around the GH-joint and the propagated external force, expressed in the local coordinate system of the humerus. Peak muscle forces were calculated as the peak of the sum of the forces applied by each muscle element, and as relative forces, by dividing them with the model-determined maximal muscle force.

Besides the RPE, input (UE-kinematics and WCP-kinetics) and outcome variables (selected output from the DSEM) were statistically tested for differences by applying a 2 by 2 factor repeated measurements Anova (Power output level (25 W and 45 W) and pre- post fatigue).

3. Results

With the fatigue protocol the RPE increased with 3.3 points to 12.1 for the 25 W condition, and with 2.4 points to 11.9 for the 45 W condition ($p = 0.000$), indicating that a higher fatigue state was obtained with the fatiguing protocol (Table 1, RPE).

In line with the hypothesis, differences in WCP-kinetics were found between the two power output conditions of 25 W and 45 W. Overall, no significant changes due to fatigue were observed in the stroke characteristics (Table 1, Propulsion kinetics). The same applied for UE-kinematics, except for thorax motion. When fatigued subjects showed more thorax movement (thorax flexion max and thorax range) (Table 1, Kinematics; Fig. 3A and 3C). No tendency was found in thorax motion (neither forward lean nor range) in dependency on lesion level (Fig. 3B and 3D).

Shoulder and elbow joint kinetics in terms of maximum moment and power differed between load conditions but did not change significantly due to fatigue (Fig. 4).

However, at the level of load at the anatomical structures of the shoulder joint, the following could be observed. Modelling results indicated a significantly higher peak glenohumeral joint contact force for the fatigued condition (Table 2). In addition, peak force contributions during the push phase were higher for the subscapularis, and deltoideus pars scapularis, but not significantly higher for the supraspinatus. This muscle was however taxed to 80 % of its peak force (Fig. 5). No interaction effects were found for power output and fatigue.

4. Discussion

Despite the higher RPE after the fatigue protocol (Fig. 1), for the two test conditions at 25 W and 45 W, no significant changes in WCP-kinetics and UE-kinematics were observed due to the fatiguing intervention, apart for thorax motion. The increased thorax forward lean in this study agreed with the studies of Rogers et al. (Rodgers et al., 1994; Rodgers et al., 2003), although they used a graded exercise test with the addition of resistance to induce exhaustion in 1994. Based on their protocol however, no distinction could be made between fatigue effects and the influence of higher resistance. Our results clearly indicated that this relationship with resistance also exists, as for the thorax both forward lean and range of motion were higher for the 45 W conditions than for the 25 W conditions. In the later study "fatigue was induced by propelling on a wheelchair ergometer at 3 km/h with a submaximal load at 75 % of peak oxygen uptake of the each participant, until volitional exhaustion" (Rodgers et al., 2003). Some differences between studies hamper a direct comparison. The propulsion velocity in the Rodgers studies was 3.5 km/h and 3 km/h versus 4 km/h in the current study. In the Rodgers study, power output was not reported per individual but likely to be in a higher range and varying over participants. In the current study power output was controlled at 25 W and 45 W. Furthermore, the linked segment models used by Rodgers calculates joint moments and powers around the thoraco-humeral joint, whereas the DSEM utilizes the glenohumeral joint. However, at group level the following can be observed: when fatigued, participants tend to use their thorax more for the propulsion, indicated by a larger thorax flexion range, and a slightly higher GH joint moment and power. They also show a slight reduction in elbow moment and power for the 45 W conditions,

Table 1
RPE, propulsion kinetics, kinematics, and joint kinetics for both power output conditions, pre and post fatigue. Data are averages over 12 subjects. Values between brackets indicate standard deviations. P-values in bold indicate significance.

	25 W pre	45 W pre	25 W post	45 W post	load	fatigue	load × fatigue
Variable name					p-value	p-value	p-value
RPE	8.8	9.5	12.1	11.9	0.087	<0.001	0.036
Propulsion kinetics							
push time [s]	0.39 (0.05)	0.41 (0.05)	0.40 (0.05)	0.40 (0.06)	0.126	0.737	0.635
cycle time [s]	0.83 (0.10)	0.75 (0.06)	0.81 (0.10)	0.76 (0.09)	**0.001**	0.991	0.249
start angle [°]	114.1 (11.9)	110.3 (9.3)	113.6 (10.2)	109.2 (9.8)	**0.022**	0.466	0.789
end angle [°]	40.1 (9.9)	34.2 (6.7)	40.2 (8.2)	33.3 (6.0)	**0.001**	0.537	0.384
total force max [N]	55.8 (13.8)	80.0 (9.2)	59.6 (11.7)	81.0 (11.3)	**<0.001**	0.291	0.274
Total hand moment max [NM]	11.9 (1.9)	17.5 (3.3)	12.0 (2.5)	17.6 (2.8)	**<0.001**	0.826	0.989
Kinematics							
thorax flexion min [°]	11.8 (6.9)	14.9 (7.0)	11.7 (7.3)	18.4 (12.5)	**0.028**	0.135	0.247
thorax flexion max [°]	25.9 (10.8)	31.9 (12.1)	27.4 (10.3)	38.6 (16.1)	**0.002**	**0.006**	0.198
thorax range [°]	14.0 (5.9)	17.0 (7.6)	15.7 (5.9)	20.2 (8.3)	**0.001**	**<0.001**	0.146
arm elevation min [°]	26.3 (3.1)	26.2 (3.6)	26.1 (3.5)	26.6 (3.5)	0.673	0.913	0.428
arm elevation max [°]	48.8 (5.3)	49.1 (5.3)	48.4 (6.3)	46.9 (5.4)	0.549	0.098	0.328
elbow flexion max [°]	89.9 (4.7)	90.9 (4.6)	91.2 (6.0)	91.8 (5.5)	0.102	0.196	0.823
elbow flexion min [°]	50.2 (12.8)	46.5 (11.8)	51.4 (11.6)	46.0 (12.2)	**0.004**	0.762	0.249
Joint Kinetics							
GH joint moment [Nm]	15.2 (4.4)	21.0 (5.3)	16.1 (3.3)	21.3 (4.7)	**<0.001**	0.516	0.709
EL joint moment [Nm]	5.6 (3.5)	9.1 (5.1)	6.3 (3.3)	8.4 (4.2)	**0.006**	0.979	0.261
GH Power [W]	69.0 (33.2)	108.9 (45.9)	79.8 (35.7)	114.2 (67.3)	**0.007**	0.522	0.818
EL Power [W]	18.9 (14.7)	36.4 (20.5)	20.0 (9.9)	33.3 (18.2)	**<0.001**	0.792	0.525

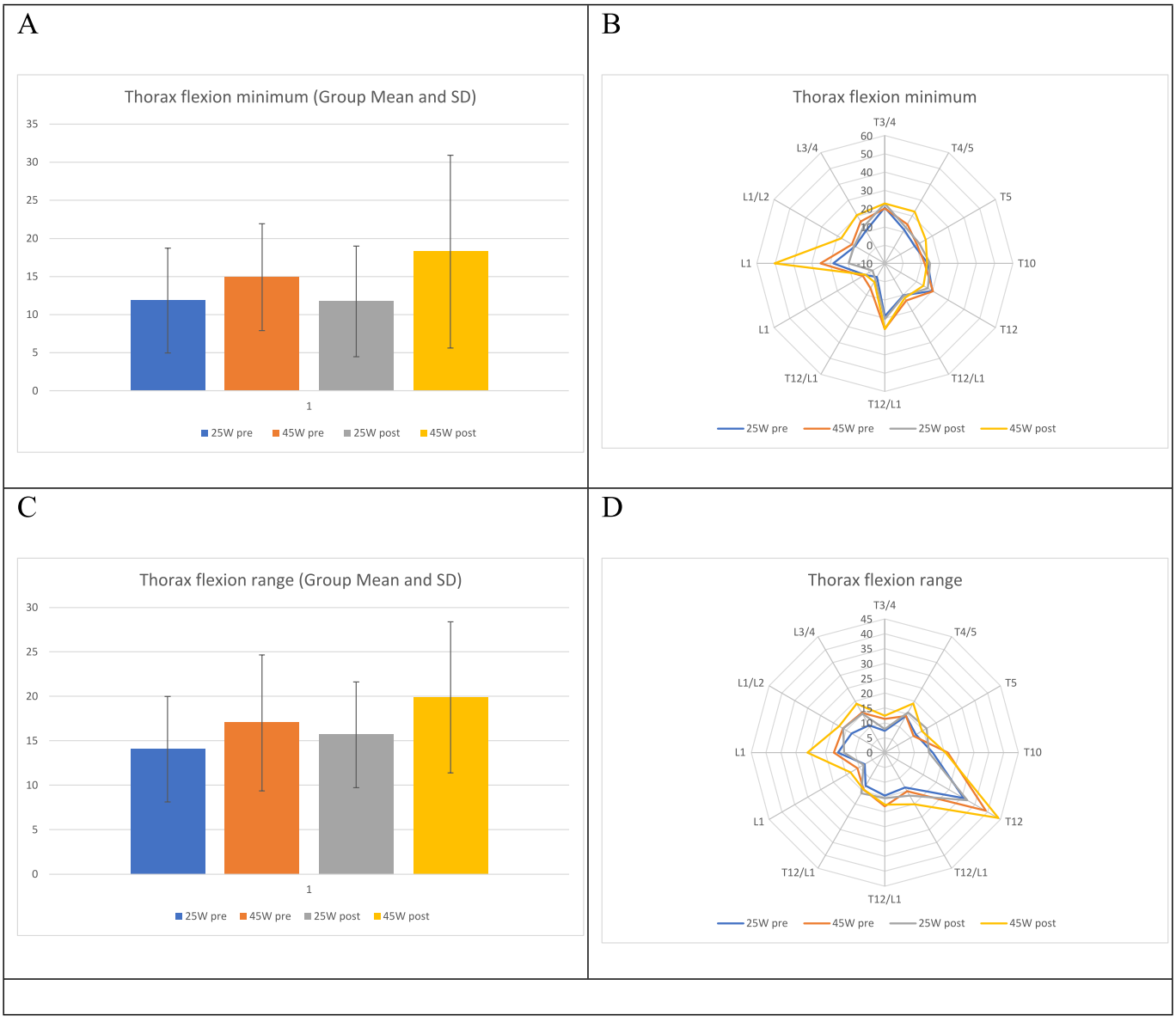

Fig. 3. Depicts the minimal thorax flexion (thorax minimal lean) averaged over participants (A), and for the 12 participants sorted on lesion level (B). thorax flexion range in (C) indicates the amount of thorax movement (group mean) during the push phase, in (D) the individual values are shown, for all 4 experimental conditions. All values are in degrees.

when fatigued. However, joint moments and powers did not show to be statistically significant different in the current study.

Although the magnitude of the presented increase in thorax range is in the order of 2 to 4 degrees (averaged values over participants), the change in force-play around the shoulder changes significantly.

Following the fatigue protocol, an increased GH contact force and increased muscle forces for subscapularis and deltoideus pars scapularis were estimated by the DSEM. This observation aligns with results from Qi et al. (Qi et al., 2021), who concluded that *'fatigue related changes in neuromuscular activity (EMG) contribute to muscle imbalance and reflect a strategy of joint stiffening'* during fatiguing wheelchair propulsion. Notably, this concordance of findings is intriguing as Qi et al. base their conclusions on disparate data sources and methodologies, utilizing surface EMG and principal component analysis (PCA) to analyze changes in muscle coordination patterns, whereas the present study employs a musculoskeletal model to estimate the mechanical variations in the force dynamics around the shoulder, up to the level of individual muscle force contributions.

Our hypothesis was that fatigue induced by the protocol would result in modifications to both the technique and the forces involved in propulsion, potentially increasing strain on the rotator cuff. Although no changes in exerted forces were observed due to fatigue, and only thorax motion changed with increased forward lean and RoM, this resulted in a higher strain on the shoulder joint and components of the rotator cuff. In the human shoulder, fatigue in some muscles (pectoralis, deltoids, and upper trapezius (Bossuyt et al., 2020a)) could cause a muscular imbalance, placing more strain on the rotator cuff for stabilization and thereby increasing the GH contact force. It seems logic to expand the musculoskeletal model and include fatigue in the cost function for the optimization of muscle forces, such is however complex to examine, validate and implement. Muscle fatigue is not only dependent on actual work and power delivered, but also on training status, nutritional status, and many other factors. A fundamental sound approach could be the simultaneous measurement of isometric elbow moment and EMG of relevant muscles and analyze the change in EMG amplitude frequency and distribution thereof, due to fatigue, to model a cost-function, per participant. This all

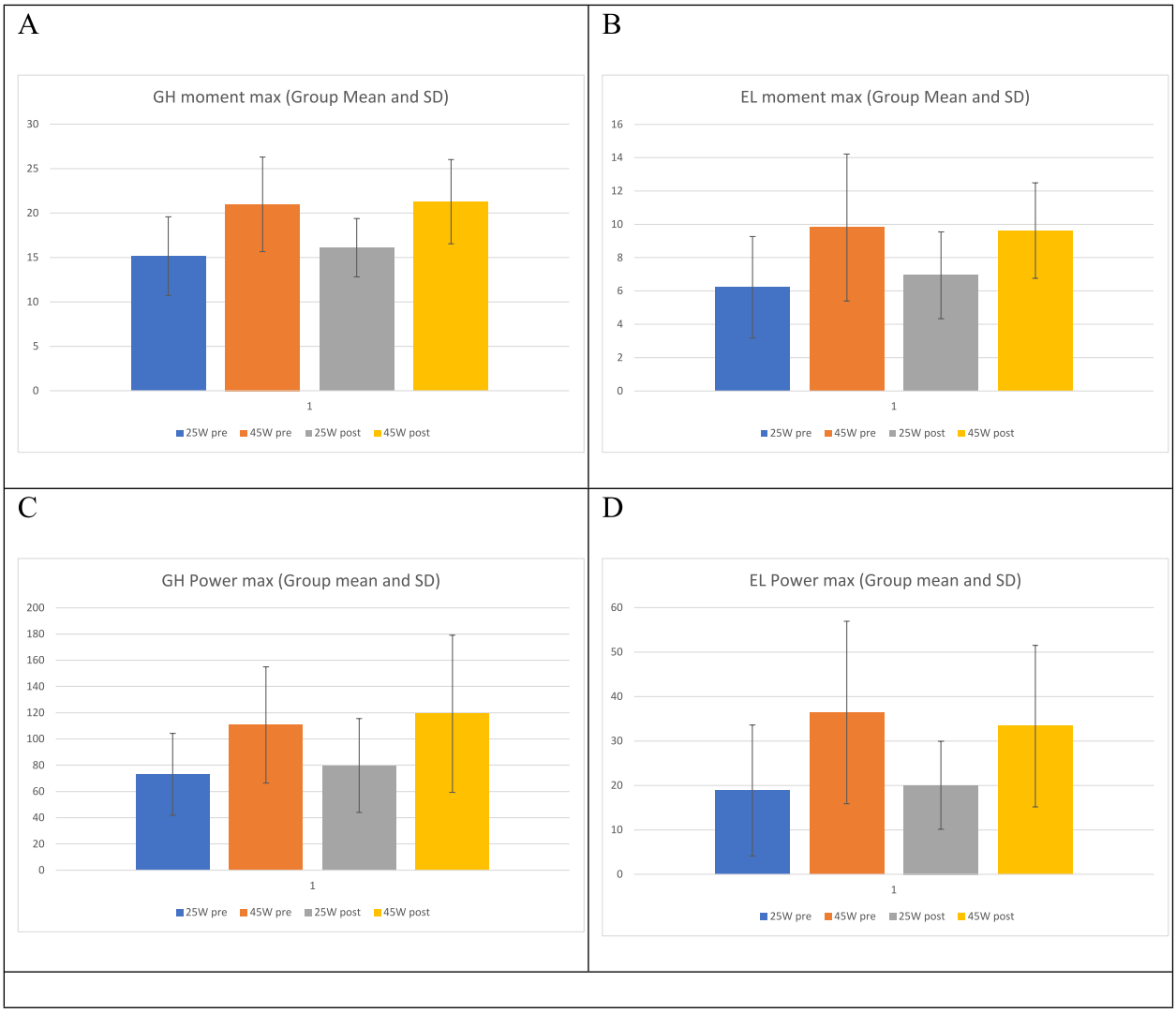

Fig. 4. Depicts the peak moment and power for the GH joint and elbow respectively. For the GH joint total moment and power are displayed, for the elbow joint the values relate to flexion. Values are group means and standard deviation thereof, for the push phase of the four conditions.

Table 2
Peak moments and forces for the glenohumeral joint before and after the fatiguing intervention, as calculated with the DSEM shoulder model. Data depicted are averages over 12 subjects, for the full propulsive cycle. Values between brackets indicate standard deviations. P-values in bold indicate significance.

	25 W before	45 W before	25 W after	45 W after	load	fatigue	load × fatigue
Variable name					p-value	p-value	p-value
Shoulder load							
GH contact force [N]	529.4 (201.0)	850.3 (495.9)	638.2 (336.2)	911.9 (382.1)	**0.001**	**0.014**	0.656
AC contact force [N]	75.7 (50.0)	131.8 (159.5)	113.6 (121.1)	147.2 (194.4)	0.158	0.133	0.276
Infraspinatus [N]	103.3 (82.8)	174.2 (152.8)	122.5 (143.9)	197.4 (155.7)	**0.001**	0.363	0.910
Teres minor [N]	8.5 (10.2)	10.1 (11.7)	7.3 (7.0)	11.3 (9.9)	0.290	1.000	0.178
Supraspinatus [N]	178.7 (61.5)	243.4 (74.4)	187.0 (69.8)	260.8 (78.5)	**<0.001**	0.155	0.666
Subscapularis [N]	207.5 (123.6)	323.3 (187.1)	248.0 (135.4)	354.8 (162.3)	**<0.001**	**0.014**	0.639
Deltoideus pars clav. [N]	20.6 (69.2)	36.5 (118.0)	52.6 (128.2)	70.4 (219.7)	0.494	0.176	0.942
Deltoideus pars scap. [N]	137.3 (48.0)	218.6 (211.2)	193.1 (144.4)	232.9 (153.2)	0.093	**0.018**	0.503
Biceps [N]	77.3 (35.2)	125.7 (113.1)	87.4 (40.9)	129.1 (78.8)	0.070	0.336	0.803
Triceps [N]	314.8 (106.2)	562.1 (338.8)	358.7 (122.3)	527.5 (274.8)	**0.031**	0.860	0.183

is, however, far beyond the scope of the current manuscript. The current DSEM just estimates the mechanical optimal result and although muscle fatigue itself is not modelled in the DSEM, the subtle but significant changes in kinematics due to fatigue do lead to an altered mechanical force-play around the shoulder, supporting the idea of compensation for fatigue with altered muscular activation.

A higher loading of the shoulder might lead to a higher risk of overuse injuries. Prospective cohort studies are required to examine if current findings do occur in real-life settings, and to further examine the relationship of higher shoulder loading and increased injury risk. Future research could investigate the hypothesis that the occurrence of trauma is intricately related to the combination of both peak and repetitive loading, as weight relief lifts or transfers, while the dependency on the upper extremity for ambulation (wheelchair propulsion) reduces the

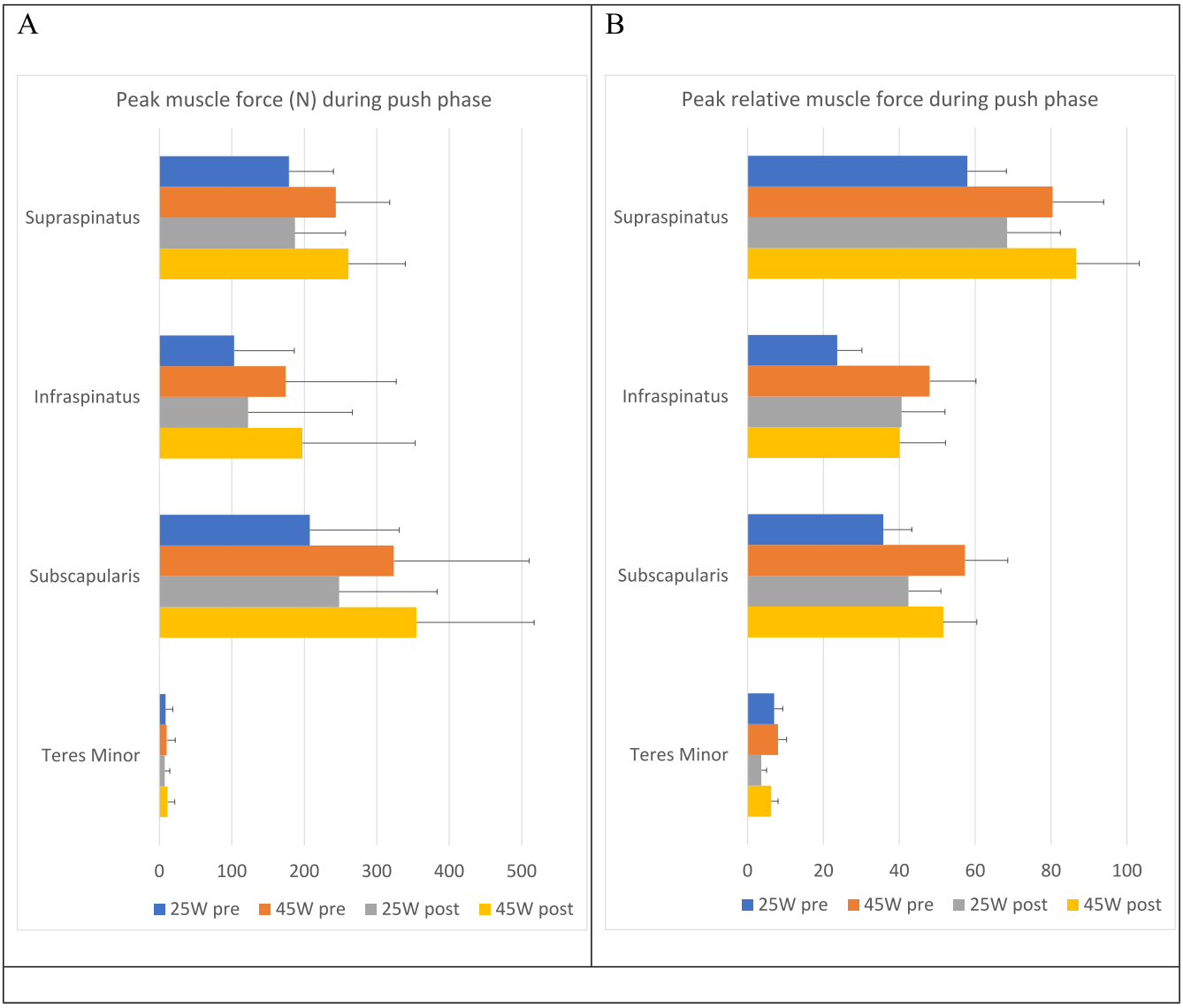

Fig. 5. A depicts the peak absolute (N) and Fig. 5B the peak relative forces (%) of the rotator cuff muscles, during the push phase, for the four conditions. Data depicted are averaged over the 12 participants.

potential for recovery. Subsequent fatigue could temporarily reduce the maximum capacity, thereby increasing the risk for trauma from peak loading activities which are inevitable during daily wheelchair life (Bossuyt et al., 2020a; Minder et al., 2023; Trigt et al., 2020).

Importantly, based on the current findings, an increase in thorax forward lean and RoM during manual wheelchair propulsion could serve as an early warning signal for fatigue.

Limitations:

The musculoskeletal model used is time-insensitive and although very interesting, fatiguing effects are not included in the cost function of the model. Such is complex to examine, implement and validate on an individual level, but could be a topic for future fundamental research, as all musculoskeletal models could benefit from such insights. Furthermore, the model is a general model and only represents group effects ignoring potential sex differences which have been observed in this data set with fatiguing propulsion previously (Bossuyt et al., 2020a; Bossuyt et al., 2020b). Furthermore, the model is not scaled towards the geometry of the participants, which can be seen as a limitation in accuracy. Instead, joint angles are scaled towards the model, to solve a mismatch between model and subject shoulder-girdle geometry. This is needed as the shoulder-girdle is a closed chain mechanism. Leaving out such optimization almost always results in situations where the scapula and/or clavicula of the model are forced to penetrate the thorax, or results in a "floating scapula", when it is no longer attached or aligned with the scapulo-thoracic gliding plane. Such segment orientations of the model are unrealistic, and result in unrealistic output. This approach is in contrast with OpenSim models of the shoulder-girdle, that scales the geometry of the model towards the measured geometry of the subjects. Although the geometrical scaling towards segment length is logic and produces more realistic joint kinetics, muscle fiber length does not scale linearly with segment or body length (Son et al., 2024). Although the latter has been shown for leg muscles, it is likely the same variation applies to upper extremity muscles. As long as this gap in knowledge exists, the scaling of musculoskeletal models will be topic of debate. Furthermore, personal responses can be, and are, of course different. We did not explore possible associations in RPE with shoulder load.

5. Conclusion

Although no significant alterations were observed in exerted forces due to fatigue, increased thorax forward lean and range of motion were observed, along with a higher strain on the shoulder joint and

components of the rotator cuff. These findings suggest a potential link between fatigue, altered propulsion technique, and increased shoulder loading, which could elevate the risk of overuse injuries. Future research is suggested to further examine the relationship of higher shoulder loading and increased injury risk. Additionally, an increase in thorax motion during wheelchair propulsion may serve as an early indicator of fatigue.

CRediT authorship contribution statement

W.H.K. de Vries: Investigation. **F.M. Bossuyt:** Writing – review & editing, Writing – original draft, Resources, Project administration, Methodology, Investigation, Formal analysis, Data curation, Conceptualization. **H.E.J. Veeger:** Investigation. **U. Arnet:** Writing – review & editing, Writing – original draft, Visualization, Validation, Supervision, Software, Resources, Project administration, Methodology, Investigation, Funding acquisition, Formal analysis, Data curation, Conceptualization.

Declaration of competing interest

The authors declare that they have no known competing financial interests or personal relationships that could have appeared to influence the work reported in this paper.

References

Akbar, M., Balean, G., Brunner, M., Seyler, T.M., Bruckner, T., Munzinger, J., Grieser, T., Gerner, H.J., Loew, M., 2010. Prevalence of rotator cuff tear in paraplegic patients compared with controls. J. Bone Joint Surg. Am. 92, 23–30.

Arnet, U., de Vries, W.H., Eriks-Hoogland, I., Wisianowsky, C., van der Woude, L.H.V., Veeger, D., Berger, M., Swi, S.C.I.S.G., 2022. MRI evaluation of shoulder pathologies in wheelchair users with spinal cord injury and the relation to shoulder pain. J. Spinal Cord Med. 45, 916–929.

Bolsterlee, B., Veeger, H.E., van der Helm, F.C., 2014. Modelling clavicular and scapular kinematics: from measurement to simulation. Med. Biol. Eng. Compu. 52, 283–291.

Bossuyt, F.M., Arnet, U., Brinkhof, M.W.G., Eriks-Hoogland, I., Lay, V., Muller, R., Sunnaker, M., Hinrichs, T., Swi, S.C.I.s.g., 2018. Shoulder pain in the Swiss spinal cord injury community: prevalence and associated factors. Disabil Rehabil 40, 798-805.

Bossuyt, F.M., Arnet, U., Cools, A., Rigot, S., de Vries, W., Eriks-Hoogland, I., Boninger, M.L., Swi, S.C.I.S.G., 2020a. Compensation strategies in response to fatiguing propulsion in wheelchair users: implications for shoulder injury risk. Am. J. Phys. Med. Rehabil. 99, 91–98.

Bossuyt, F.M., Boninger, M.L., Cools, A., Hogaboom, N., Eriks-Hoogland, I., Arnet, U., Swi, S.C.I.s.g., 2020b. Changes in supraspinatus and biceps tendon thickness: influence of fatiguing propulsion in wheelchair users with spinal cord injury. Spinal Cord 58, 324-333.

Chamberlain, J.D., Meier, S., Mader, L., von Groote, P.M., Brinkhof, M.W., 2015. Mortality and longevity after a spinal cord injury: systematic review and meta-analysis. Neuroepidemiology 44, 182–198.

Collinger, J.L., Impink, B.G., Ozawa, H., Boninger, M.L., 2010. Effect of an intense wheelchair propulsion task on quantitative ultrasound of shoulder tendons. PM R 2, 920–925.

Dubowsky, S.R., Rasmussen, J., Sisto, S.A., Langrana, N.A., 2008. Validation of a musculoskeletal model of wheelchair propulsion and its application to minimizing shoulder joint forces. J. Biomech. 41, 2981–2988.

Eriks-Hoogland, I.E., de Groot, S., Post, M.W., van der Woude, L.H., 2011. Correlation of shoulder range of motion limitations at discharge with limitations in activities and participation one year later in persons with spinal cord injury. J Rehabil Med 43, 210–215.

Gagnon, D., Nadeau, S., Noreau, L., Dehail, P., Piotte, F., 2008. Comparison of peak shoulder and elbow mechanical loads during weight-relief lifts and sitting pivot transfers among manual wheelchair users with spinal cord injury. J. Rehabil. Res. Dev. 45, 863–873.

Gironda, R.J., Clark, M., Neugaard, B., Nelson, A., 2004. Upper limb pain in Anational sample of veterans with paraplegia. J. Spinal Cord Med. 27, 120–127.

Gutierrez, D.D., Thompson, L., Kemp, B., Mulroy, S.J., Physical Therapy Clinical Research, N., Rehabilitation, R., Training Center on Aging-Related Changes in Impairment for Persons Living with Physical, D., 2007. The relationship of shoulder pain intensity to quality of life, physical activity, and community participation in persons with paraplegia. J Spinal Cord Med 30, 251-255.

Holloway, C.S., Symonds, A., Suzuki, T., Gall, A., Smitham, P., Taylor, S., 2015. Linking wheelchair kinetics to glenohumeral joint demand during everyday accessibility activities. Annu. Int. Conf. IEEE Eng. Med. Biol. Soc. 2015, 2478–2481.

Jensen, M.P., Hoffman, A.J., Cardenas, D.D., 2005. Chronic pain in individuals with spinal cord injury: a survey and longitudinal study. Spinal Cord 43, 704–712.

Karduna, A.R., McClure, P.W., Michener, L.A., Sennett, B., 2001. Dynamic measurements of three-dimensional scapular kinematics: a validation study. J. Biomech. Eng. 123, 184–190.

Leving, M.T., Vegter, R.J.K., de Vries, W.H.K., de Groot, S., van der Woude, L.H.V., 2018. Changes in propulsion technique and shoulder complex loading following low-intensity wheelchair practice in novices. PLoS One 13, e0207291.

Lin, H.T., Su, F.C., Wu, H.W., An, K.N., 2004. Muscle forces analysis in the shoulder mechanism during wheelchair propulsion. Proc. Inst. Mech. Eng. H 218, 213–221.

McClure, P.W., Michener, L.A., Sennett, B.J., Karduna, A.R., 2001. Direct 3-dimensional measurement of scapular kinematics during dynamic movements in vivo. Journal of shoulder and elbow surgery / American Shoulder and Elbow Surgeons ... [et al.] 10, 269-277.

Meskers, C.G., van de Sande, M.A., de Groot, J.H., 2007. Comparison between tripod and skin-fixed recording of scapular motion. J. Biomech. 40, 941–946.

Minder, U., Arnet, U., Muller, E., Boninger, M., Bossuyt, F.M., 2023. Changes in neuromuscular activation, heart rate and rate of perceived exertion over the course of a wheelchair propulsion fatigue protocol. Front. Physiol. 14, 1220969.

Nikooyan, A.A., Veeger, H.E., Chadwick, E.K., Praagman, M., Helm, F.C., 2011. Development of a comprehensive musculoskeletal model of the shoulder and elbow. Med. Biol. Eng. Compu. 49, 1425–1435.

Nikooyan, A.A., Veeger, H.E., Westerhoff, P., Graichen, F., Bergmann, G., van der Helm, F.C., 2010. Validation of the Delft Shoulder and Elbow Model using in-vivo glenohumeral joint contact forces. J. Biomech. 43, 3007–3014.

Praagman, M., Chadwick, E.K., van der Helm, F.C., Veeger, H.E., 2006. The relationship between two different mechanical cost functions and muscle oxygen consumption. J. Biomech. 39, 758–765.

Qi, L., Guan, S., Zhang, L., Liu, H.L., Sun, C.K., Ferguson-Pell, M., 2021. The effect of fatigue on wheelchair users' upper limb muscle coordination patterns in time-frequency and principal component analysis. IEEE Trans. Neural Syst. Rehabil. Eng. 29, 2096–2102.

Rice, I., Impink, B., Niyonkuru, C., Boninger, M., 2009. Manual wheelchair stroke characteristics during an extended period of propulsion. Spinal Cord 47, 413–417.

Rodgers, M.M., Gayle, G.W., Figoni, S.F., Kobayashi, M., Lieh, J., Glaser, R.M., 1994. Biomechanics of wheelchair propulsion during fatigue. Arch. Phys. Med. Rehabil. 75, 85–93.

Rodgers, M.M., McQuade, K.J., Rasch, E.K., Keyser, R.E., Finley, M.A., 2003. Upper-limb fatigue-related joint power shifts in experienced wheelchair users and nonwheelchair users. J. Rehabil. Res. Dev. 40, 27–37.

Son, J., Ward, S.R., Lieber, R.L., 2024. Scaling relationships between human leg muscle architectural properties and body size. J. Exp. Biol. 227.

Strauss, D.J., Devivo, M.J., Paculdo, D.R., Shavelle, R.M., 2006. Trends in life expectancy after spinal cord injury. Arch. Phys. Med. Rehabil. 87, 1079–1085.

Trigt, B.v., Leenen, T., Hoozemans, M., Helm, F.v.d., Veeger, D., 2020. Are UCL Injuries a Matter of Bad Luck? The Role of Variability and Fatigue Quantified, The 13th Conference of the International Sports Engineering Association.

Turner, J.A., Cardenas, D.D., Warms, C.A., McClellan, C.B., 2001. Chronic pain associated with spinal cord injuries: a community survey. Arch. Phys. Med. Rehabil. 82, 501–509.

van Andel, C.J., Wolterbeek, N., Doorenbosch, C.A., Veeger, D.H., Harlaar, J., 2008. Complete 3D kinematics of upper extremity functional tasks. Gait Posture 27, 120–127.

van der Helm, F.C., 1994a. Analysis of the kinematic and dynamic behavior of the shoulder mechanism. J. Biomech. 27, 527–550.

van der Helm, F.C., 1994b. A finite element musculoskeletal model of the shoulder mechanism. J. Biomech. 27, 551–569.

van der Helm, F.C., Veeger, H.E.J., 1999. Shoulder modelling in rehabilitation: The power balance during wheelchair propulsion. In: van der Woude, L.H.V., Hopman, M.T.E., Van Kemenade, C.H. (Eds.), Biomedical Aspects of Manual Wheelchair Propulsion. The State of the Art II. IOS Press, Amsterdam, pp. 96-103.

van der Linden, M.L., Valent, L., Veeger, H.E., van der Woude, L.H., 1996. The effect of wheelchair handrim tube diameter on propulsion efficiency and force application (tube diameter and efficiency in wheelchairs). IEEE Trans. Rehabil. Eng. 4, 123–132.

van Drongelen, S., van der Woude, L.H., Veeger, H.E., 2011. Load on the shoulder complex during wheelchair propulsion and weight relief lifting. Clin. Biomech. (Bristol, Avon) 26, 452–457.

Veeger, H.E., Rozendaal, L.A., van der Helm, F.C., 2002. Load on the shoulder in low intensity wheelchair propulsion. Clin. Biomech. (Bristol, Avon) 17, 211–218.

Veeger, H.E., Van der Helm, F.C., Van der Woude, L.H., Pronk, G.M., Rozendal, R.H., 1991. Inertia and muscle contraction parameters for musculoskeletal modelling of the shoulder mechanism. J. Biomech. 24, 615–629.

Veeger, H.E., Yu, B., An, K.N., Rozendal, R.H., 1997. Parameters for modeling the upper extremity. J. Biomech. 30, 647–652.

Wu, G., van der Helm, F.C., Veeger, H.E., Makhsous, M., Van Roy, P., Anglin, C., Nagels, J., Karduna, A.R., McQuade, K., Wang, X., Werner, F.W., Buchholz, B., International Society of, B., 2005. ISB recommendation on definitions of joint coordinate systems of various joints for the reporting of human joint motion–Part II: shoulder, elbow, wrist and hand. J Biomech 38, 981-992.